Effect of optical purity on phase sequence in antiferroelectric liquid crystals

Nataša Vaupotič[1,2] and Mojca Čepič[1,3]
[1]*Institut Jozef Stefan, Ljubljana, Slovenia*
[2]*Department of Physics, Faculty of Education, University of Maribor, Maribor, Slovenia*
[3]*Department of Physics, Faculty of Education, University of Ljubljana, Ljubljana, Slovenia*
(Received 17 September 2004; published 4 April 2005)

We use the discrete phenomenological model to study theoretically the phase diagrams in antiferroelectric liquid crystals (AFLCs) as a function of optical purity and temperature. High sensitivity of the phase sequence in the AFLCs to optical purity is attributed to the piezoelectric coupling which is reduced if optical purity is reduced. We limit our study to three topologically equal smetic (Sm)phases: Sm-C^*, Sm-C^*_α, and Sm-C^*_A and show that the reduction of optical purity forces the system from the antiferroelectric to the ferroelectric phase with a possible Sm-$C^\star_\alpha$ between them. The effect of the flexoelectric and the quadratic coupling is considered as well. If the phase diagram includes only two phases, Sm-$C^\star$ and Sm-$C^\star_A$, the flexoelectric coupling is very small. The materials which exhibit the Sm-$C^\star_\alpha$ in a certain range of optical purity and temperature, can be expected to have a significant flexoelectric coupling that is comparable with the piezoelectric coupling. Upon lowering the temperature the phase sequence Sm-$A \rightarrow$ Sm-$C^\star_\alpha \rightarrow$ Sm-$C^\star \rightarrow$ Sm-$C^\star_A$ is possible in systems where quadratic coupling is very strong.

DOI: 10.1103/PhysRevE.71.041701 PACS number(s): 61.30.Cz, 64.70.Md

I. INTRODUCTION

Antiferroelectric liquid crystals (AFLCs) were discovered more than 15 years ago when macroscopic properties of mixtures of left- and right-handed MHPOBC, nowadays known as a prototype antiferroelectric liquid crystal, were studied [1]. Scientists were surprised at the rich variety of phases found in these systems and at the influence that the optical purity has on the phase sequence. There is a number of phenomena found in these complex systems [2–6] and the macroscopic properties of some of the phases were explained only recently by the phenomenological theoretical modeling [7].

In chiral antiferroelectric liquid crystals there always exists at least one phase with antiferroelectric properties, the smectic-C^*_A phase (Sm-C^*_A). Due to the oppositely (anticlinically) tilted elongated molecules in the neighboring layers, the piezoelectrically induced polarization is cancelled out and the system behaves antiferroelectrically in the external electric field. The structure is additionally helicoidally modulated by a double helix formed from anticlinically tilted layers. The length of the pitch depends on optical purity and it is infinite in racemic mixtures. The synclinically tilted ferroelectric Sm-C^* phase is also often found in AFLCs. It is stable at higher temperatures than the Sm-C^*_A phase. In the temperature range between the Sm-C^*_A and the Sm-C^* phase two other phases with a short modulation over 3 and 4 layers and long helicoidal modulation over at least few hundred of layers can exist [6]. They are called Sm-$C^*_{FI,I}$ and Sm-$C^*_{FI,II}$, respectively. In optically very pure samples the 4-layer phase is sometimes stable within the same temperature range as the Sm-C^* phase [8]. Directly below the transition to the tilted phase, the phase called Sm-C^*_α can be stable. This phase is topologically equal to the Sm-C^* phase (which means that the translation for one layer plus the rotation for the phase angle around the layer normal is the symmetry operation) but the period of the helicoidal modulation extends over a few layers only. The phase transition between the Sm-C^*_α and Sm-C^* is of an isostructural type and can be recognized by differential calorimetry measurements only if the changes of the properties like the length of the modulation period or the tilt magnitude is abrupt [9]. More exact measurements like simultaneous measurements of optical rotatory power and the tilt [10] have shown that the Sm-C^*_α phase exists also at lower optical purities but transforms continuously to the structure of the Sm-C^* phase with a very rapid change of modulation period within an extremely narrow temperature range (a few mK) [11].

Optical purity has a strong influence on the phase sequence. The effect was first studied before a decade and a most interesting result was observed. Until then it was generally believed that the number of phases increases with increasing optical purity and that the Sm-$C^\star_\alpha$ can exist only in optically pure samples. The experiments showed, however, that in some materials the Sm-$C^\star_\alpha$ phase does not exist in optically pure samples, but it can be observed if optical purity is reduced [12]. Since these measurements did not receive an adequate explanation for a decade the scientists from this field were challenged to search for the explanation [13]. Recently this high sensitivity of AFLCs to optical purity has been attributed to changes in smectic order [14].

In this paper we offer a different mechanism that may also contribute to the observed behavior. We account for the described properties of the phase diagram of antiferroelectric liquid crystals within the framework of the discrete phenomenological model. We limit our consideration to the phase diagrams of three topologically equal phases, also called the clock phases, Sm-C^*, Sm-C^*_α, and Sm-C^*_A, that all have helicoidally modulated structures with modulation periods of a few hundred layers, of a few layers, and of approximately two layers, respectively. All three phases may appear directly below the nontilted Sm-*A* phase. Experimentally three differ-

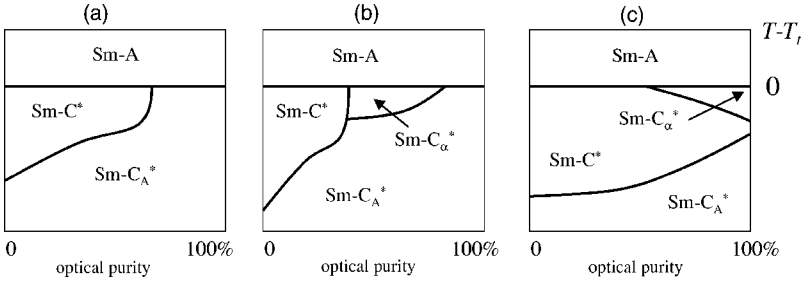

FIG. 1. Schematic drawings of the three typical phase diagrams observed in AFLCs. Only the clock phases are shown, the Sm-$C^*_{FI,I}$ and Sm-$C^*_{FI,II}$ phases are omitted. (a) TFMHPOBC, (b) TFMHPOCBC, and (c) MHPOBC.

ent phase diagrams have been observed [12,15,16], which are presented schematically in Fig. 1. The aim of our study is to show that interactions due to the chiral molecular symmetry might be responsible for the observed macroscopic behavior. The plan of the paper is the following. First we present the discrete phenomenological model and discuss the theoretical predictions on how optical purity affects the phase sequence. Then we present theoretically obtained phase diagrams in which stability regions of phases are shown as a function of temperature and optical purity. Finally we discuss the results and draw the conclusions.

II. MODEL

We use the discrete phenomenological model [17] and write the free energy of the system in terms of the tilt vector $\boldsymbol{\xi}_j$ and the polar order parameter $\boldsymbol{\eta}_j$ (see Fig. 2) in the jth smectic layer. The tilt vector is the projection of the director $\mathbf{n}$ to the smectic plane and its magnitude is equal to the tilt ϑ. The spontaneous polarization in the jth layer is proportional to the polar order parameter: $\mathbf{P}_j = P_0 \boldsymbol{\eta}_j$, where P_0 is the polarization of the completely polarly ordered layer [18]. Because of that the polar order parameter will be referred to as *polarization*.

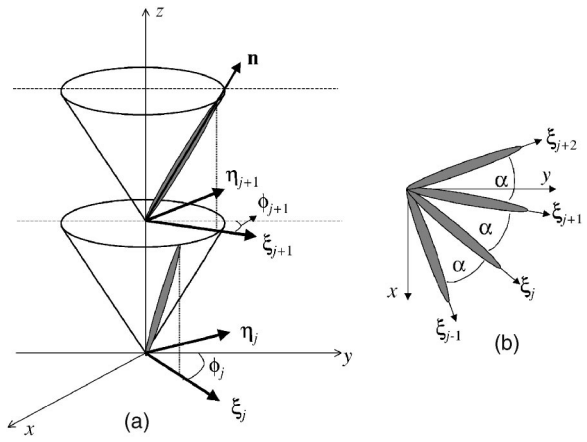

FIG. 2. The geometry of the problem and the definition of the order parameters. (a) Smectic layers run along the z direction. Molecules lie on the tilt cone; the magnitude of the tilt is ϑ. The system is described by two order parameters: $\boldsymbol{\xi}_j$ and $\boldsymbol{\eta}_j$. The tilt vector $\boldsymbol{\xi}_j$ points in the direction of the projection of the director $\mathbf{n}$ to the smectic plane (the xy plane). Its magnitude is ϑ. The phase angle between the tilt vector in the jth and the $(j+1)$th layer is $\phi_{j+1} - \phi_j = \alpha$ and it is constant. In the Sm-$C^\star$ phase $\alpha \approx 0$ and in the Sm-$C^\star_A$ phase $\alpha \approx \pi$. The polar order parameter $\boldsymbol{\eta}_j$ lies in the smectic plane and it is perpendicular to the tilt vector. (b) Top view on the layers. The ellipse now presents the projection of the molecule on the smectic plane.

The free energy of the smectic system with N layers is

$$
\begin{aligned}
G = a\sum_{j=1}^{N} & \frac{1}{2}(T - T_0)\boldsymbol{\xi}_j^2 + \frac{1}{4}b\boldsymbol{\xi}_j^4 + \frac{1}{2}a_{10}(\boldsymbol{\xi}_j \cdot \boldsymbol{\xi}_{j+1}) \\
& + \frac{1}{2}a_{11}\boldsymbol{\xi}_j^2(\boldsymbol{\xi}_j \cdot \boldsymbol{\xi}_{j+1}) + \frac{1}{2}b_Q(\boldsymbol{\xi}_j \cdot \boldsymbol{\xi}_{j+1})^2 + \frac{1}{2}f_1(\boldsymbol{\xi}_j \times \boldsymbol{\xi}_{j+1})_z \\
& + \frac{1}{2}b_0\boldsymbol{\eta}_j^2 + \frac{1}{2}b_1(\boldsymbol{\eta}_j \cdot \boldsymbol{\eta}_{j+1}) + \frac{1}{8}b_2(\boldsymbol{\eta}_j \cdot \boldsymbol{\eta}_{j+2}) + c_p(\boldsymbol{\eta}_j \times \boldsymbol{\xi}_j)_z \\
& + \frac{1}{2}\mu(\boldsymbol{\xi}_{j-1} - \boldsymbol{\xi}_{j+1}) \cdot \boldsymbol{\eta}_j. \qquad (1)
\end{aligned}
$$

The terms written are the lowest order terms allowed by the symmetry of the chiral smectic phase. The first two terms in Eq. (1) describe the phase transition from the nontilted to the tilted phase, which in an isolated layer occurs at $T = T_0$. Interactions with neighboring layers increase the phase transition temperature to $T_t > T_0$. The four terms in the second line of the Eq. (1) describe the coupling among the tilts in the neighboring layers. This coupling can prefer either synclinic or anticlinic ordering of the tilts so the parameter a_{10} can be either negative or positive, respectively. The a_{11} term, which depends on the magnitude of the tilt, describes the effect that with the increasing tilt the anticlinic ordering in the neighboring layers becomes more favorable. The quadratic coupling (b_Q) equally favors synclinic and anticlinic ordering in the neighboring layers [19,20], so b_Q is negative. The term f_1 is the discrete analog of the Lifshitz term and reflects the chiral symmetry of the phase.

The parameters b_0, b_1, and b_2 give the electrostatic interaction among the permanent dipoles inside the layer, between the nearest layers and the next nearest layers, respectively. It was shown [21] that the electrostatic interaction between the next nearest layers does not significantly affect the structure, so in the rest of the paper we set $b_2 = 0$. Since polar order is induced by the tilt, it does not behave critically and therefore b_0 is always positive. The parameter b_1 is also positive, because for elongated molecules with transverse dipoles the electrostatic interaction between the neigboring layers always favors antiferroelectric ordering [22]—the system can, of course, still be in a ferroelectric phase if $a_{10} < 0$.

The last two terms in Eq. (1) are the coupling terms between the tilt and polarization. The piezoelectric coupling (given by c_p) decribes the effect that the rotation around the director **n** is hindered in tilted phases. In chiral systems this leads to the macroscopic polarization of the smectic layer in the direction perpendicular to the tilt. If the tilts in the layers next to the considered layer are different this affects the hindrance of rotation in the considered layer and as a consequence the layer polarization changes. This effect is called flexoelectric coupling and is given by the term with the parameter μ.

All the parameters are given in the units of K, except the parameter a, which has the unit J m^{-3} K^{-1}.

Although the model is phenomenological and the vectors $\boldsymbol{\xi}_j$ and $\boldsymbol{\eta}_j$ define the average orientation of the tilt vector and the average polarization, respectively, in the whole layer, the physical significance of the terms in the free energy [Eq. (1)] can be understood from the microscopic point of view. The magnitudes of the phenomenological parameters and their sign essentially depend on the molecular structure and therefore on the interplay of the entropic effects and the intra and interlayer steric and electrostatic interactions among the constituent molecules. Steric interactions are attractive due to the induced dipole-dipole interaction or repelling due to the excluded volume effects. The electrostatic interactions are due to the permanent dipoles. Excluded volume steric interactions between the nearest layers prefer synclinic while the attractive steric interactions prefer anticlinic ordering of the long molecular axes. When temperature reduces, the interlayer molecular diffusion decreases, the excluded volume effect becomes less important and as a result the attractive steric interactions prevail which leads to anticlinic ordering. In general the molecules are not cylindrical but are to some extent flattened. In the scope of the generalized molecular asymmetry model [19,23,24] steric quadrupole can be assigned to this molecular asymmetry and if it is large enough such molecules equally like synclinic or anticlinic ordering in the neigboring layers.

We assume that the phenomenological parameters entering the model are temperature independent. Their magnitude is, however, affected by the optical purity of the sample. The parameter x is chosen as a measure for optical purity. In pure samples $x=1$ and in a racemic sample $x=0$. The change in optical purity has a pronounced effect on the magnitude of the parameters f_1 and c_p that reflect the chiral symmetry. We assume that they reduce linearly with reduced optical purity since in the racemized sample they are both essentially zero. So we write $c_p=xc_{p0}$ and $f_1=xf_{10}$. The rest of the terms can have only an even power dependence on optical purity and have a nonzero value in the racemic mixture. The main dependence on the optical purity is in the chiral terms and because of that the effect of optical purity on the rest of the parameters is neglected.

In this paper we focus only on the clock structures where the polarization ($\boldsymbol{\eta}_j$) is perpendicular to the tilt vector and the angle between the tilt vectors in the neighboring layers is constant and equal to α. In this case the free energy [Eq. (1)] can be expressed as

$$G = a\sum_{j=1}^{N} \frac{1}{2}(T-T_0)\vartheta^2 + \frac{1}{4}b\vartheta^4 + \frac{1}{2}a_{10}\vartheta^2\cos\alpha + \frac{1}{2}a_{11}\vartheta^4\cos\alpha + \frac{1}{2}b_Q\vartheta^4\cos^2\alpha + \frac{1}{2}f_1\vartheta^2\sin\alpha + \frac{1}{2}b_0\eta^2 + \frac{1}{2}b_1\eta^2\cos\alpha - c_p\vartheta\eta - \mu\vartheta\eta\sin\alpha. \quad (2)$$

When the free energy [Eq. (2)] is minimized with respect to the magnitude of the polar order parameter η, we find

$$\eta = \frac{(c_p + \mu\sin\alpha)\vartheta}{b_0 + b_1\cos\alpha}. \quad (3)$$

The polarization inside one layer thus increases with increasing tilt. The polarization also depends on the optical purity, since the piezoelectric coupling (c_p) increases with increasing optical purity.

Elimination of the polar order parameter from Eq. (2) leads to the free energy expressed only in tilt vectors:

$$G/a = \sum_{j=1}^{N} \frac{1}{2}(T-T_0)\vartheta^2 + \frac{1}{4}b\vartheta^4 + \frac{1}{2}a_{11}\vartheta^4\cos\alpha + \frac{1}{2}b_Q\vartheta^4\cos^2\alpha + \frac{1}{2}\sum_{i=1}^{4}\tilde{a}_i\vartheta^2\cos(i\alpha) + \frac{1}{2}\sum_{i=1}^{3}\tilde{f}_i\vartheta^2\sin(i\alpha).$$

The electrostatic interaction mediates the indirect coupling among the layers which extends up to the fourth-nearest layer. The whole set of the effective achiral ($\tilde{a}_i$) and chiral ($\tilde{f}_i$) parameters is given in [17]. The effective parameters between the nearest and the next nearest layers determine the type of the clock phase (Sm-$C^{\star}_{\alpha}$, Sm-$C^{\star}_{A}$, or Sm-$C^{\star}$). The couplings up to the third and the fourth nearest layers are important only when phases Sm-$C^{*}_{FI,I}$ and Sm-$C^{*}_{FI,II}$ need to be considered. Although in the numerical calculations we have included the whole set of the effective parameters, we have checked that $\tilde{a}_3$, $\tilde{a}_4$, and $\tilde{f}_3$ actually have no influence on the phase diagrams when only clock structures are considered. Because of that we discuss in more detail only the effective parameters between the nearest and the next-nearest neighboring layers:

$$\tilde{a}_1 = a_{10} + \left(\frac{c_p^2}{b_0} + \frac{\mu^2}{4b_0}\right)\frac{b_1}{b_0}, \quad (4)$$

$$\tilde{a}_2 = -\frac{c_p^2}{2b_0}\frac{b_1^2}{b_0^2} + \frac{\mu^2}{2b_0}, \quad (5)$$

$$\tilde{f}_1 = f_1 + \frac{2c_p\mu}{b_0}\left(1 + \frac{b_1^2}{4b_0^2}\right), \quad (6)$$

$$\tilde{f}_2 = -\frac{c_p \mu}{b_0}\frac{b_1}{b_0}. \tag{7}$$

The type of the structure (Sm-$C^\star$ or Sm-$C_A^\star$) depends mainly on the sign and the magnitude of the parameter $\tilde{a}_1$. If it is negative, synclinic ordering between the neighboring layers is favored, and anticlinic ordering is favored if it is positive. The second term in $\tilde{a}_1$ [see Eq. (4)] is always positive, since b_0 and b_1 are always positive, and its magnitude increases if optical purity (and thus c_p) increases. The parameter a_{10} can be either positive or negative. But even if it is negative ($a_{10}<0$) the effective coupling (described by $\tilde{a}_1$) might be such that the anticlinic ordering between the nearest layers is preferred, providing that the effect of piezo- and flexoelectric coupling **(**the second term in $\tilde{a}_1$ [see Eq. (4)]**)** is large enough to overrun the direct coupling term between the tilts in the neighboring layers. This means, that in materials in which c_{p0} is large enough, the reduction of optical purity drives the system from the antiferroelectric to the ferroelectric state.

In materials where the effective achiral coupling between the next-nearest layers ($\tilde{a}_2$) is positive, this coupling favors anticlinic ordering between the next nearest layers. This ordering is in contradiction with both the synclinic and the anticlinic ordering in the nearest layers and it enforces the stability of the Sm-$C_\alpha^\star$ phase if the condition $4|\tilde{a}_1|<\tilde{a}_2$ is satisfied [17]. If upon reduction of the optical purity the effective achiral coupling between the nearest layers changes sign, the stability condition for the Sm-$C_\alpha^\star$ phase is bound to be satisfied in a certain range of optical purity and the following phase sequence can be observed when optical purity is reduced: Sm-$C_A^\star \rightarrow$ Sm-$C_\alpha^\star \rightarrow$ Sm-$C^\star$.

We finally discuss the case of a_{10} being positive. In this case the effective parameter $\tilde{a}_1$ is positive at all optical purities, only its magnitude changes. In such system only Sm-$C_A^\star$ and Sm-$C_\alpha^\star$ can exist. The phenomenological parameters might be such that at high enough temperatures and at low enough optical purity the condition $4\tilde{a}_1<\tilde{a}_2$ is satisfied and then the system is in the Sm-$C_\alpha^\star$ phase, otherwise it will be in the Sm-$C_A^\star$ phase. The phase diagrams shown in Fig. 1 can be observed only in systems where $a_{10}<0$ and in the rest of the paper we focus on such systems.

III. THEORETICAL PHASE DIAGRAMS

The aim of this work was to obtain theoretically the phase diagrams that qualitatively agree with the experimental phase diagrams, shown in Fig. 1. Following that goal we use the model presented above and discuss the effect that changes in optical purity have on the phase diagram. We also discuss the effect of the quadratic and the flexoelectric coupling. Finally we show that by looking at the specific characteristics of the experimental phase diagram one can predict which couplings are most important in a given material.

First we focus on the effect of the piezoelectric coupling (c_p) and set the flexoelectric (μ) and the quadratic coupling (b_Q) to zero. In this case only three effective interlayer parameters ($\tilde{a}_1=a_{10}+c_p^2 b_1/b_0^2$, $\tilde{a}_2=-c_p^2 b_1^2/(2b_0^3)$ and $\tilde{f}_1=f_1$) are different from zero. There is no frustration between the nearest and the next nearest layer interactions ($\tilde{a}_2$ is negative) so a very simple phase diagram, containing only the Sm-$C_A^\star$ phase and the Sm-$C^\star$ phase, is expected. When the chiral model parameter f_{10} is very small the phase diagram is indeed simple [see Fig. 3(a)]. This diagram qualitatively agrees with the phase diagram in Fig. 1(a). However, if f_{10} is increased, the helicoidal modulation can become so large, that the structure might be recognized as the Sm-C_α^* phase. The phase angle increases continuously when temperature is lowered. In Fig. 3(a) we show the region of optical purity and temperature in which the phase angle α is greater than 0.2. This modulation [see the inset to Fig. 3(a)] is already so large that the phase might be recognized as the Sm-C_α^* phase.

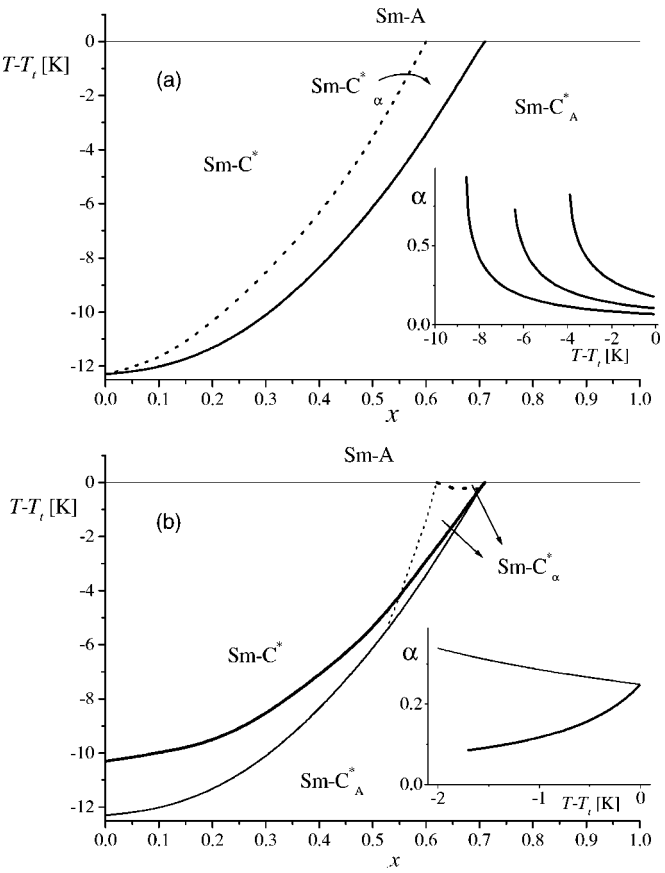

FIG. 3. Phase diagrams if no flexoelectric coupling is present. (a) $b_Q=0$; without the dotted line: $f_1=-0.01x$, with the dotted line: $f_1=-0.05x$; the inset: temperature dependence of the phase angle α in the Sm-$C_\alpha^\star$ and the Sm-$C^\star$ phase; from left to right: $x=0.4, 0.5, 0.6$. (b) $f_1=-0.05x$; the inset: $\alpha(T)$ in the Sm-$C_\alpha^\star$ and the Sm-$C^\star$ phase at $x=0.65$; thin dotted and solid line: $b_Q=-1$; thick dotted and solid line: $b_Q=-10$. Solid and dotted lines on the phase diagrams denote the discontinuous and the continuous transitions, respectively. The Sm-$C_\alpha^\star$ phase is designated to the region in which $\alpha>0.2$. The common set of parameters: $\mu=0$, $c_p=4x$, $b=120$, $a_{10}=-0.4$, $a_{11}=4$, $b_0=2$, and $b_1=b_0/10$. All the parameters are given in the units of kelvin. T_t is the transition temperature to the tilted phase.

Next we include the quadratic coupling (b_Q), which tends to stabilize synclinic or anticlinic phases. The presence of small quadratic coupling reduces the region of stability of the Sm-$C_\alpha^\star$ phase significantly as seen in Fig. 3(b). This phase

diagram qualitatively agrees with the phase diagram shown in Fig. 1(b). At even larger quadratic coupling the Sm-$C^\star$ phase "grows" into the region of the Sm-$C^\star_\alpha$ phase and the Sm-$C^\star_\alpha$ phase is almost expelled from the phase diagram as seen in Fig. 3(b).

The diagrams shown in Fig. 3 can be used to predict how a phase diagram for the material which has stronger or weaker piezoelectric coupling looks like. If, for example, the piezoelectric coupling c_{p0} is reduced by a factor of 1.5, the new phase diagram would be obtained by a simple rescaling of the optical purity x, which should be multiplied by the same factor, i.e., by 1.5. So, in this case the region of stability of the Sm-$C^\star$ phase would extend to higher optical purity, in the chosen example to $x>1$. In the case of the very strong quadratic coupling the rescaled phase diagram of Fig. 3(b) qualitatively agrees with the phase diagram in Fig. 1(c).

Let us emphasize that when the flexoelectric coupling is negligibly small the Sm-C^*_α phase is obtained solely due to the strong chiral twist. However, it is more likely that the main origin of the Sm-$C^\star_\alpha$ phase is the frustration between the nearest and the next nearest layer achiral coupling ($\tilde{a}_2>0$). This frustration is possible only in materials in which flexoelectric coupling (μ) is important. So in the rest of the section we discuss the effect of the flexoelectric coupling in more detail.

The flexoelectric coupling has several effects. As already mentioned it changes the effective coupling between the next nearest layers [see Eq. (5)] so that anticlinic ordering is preferred ($\tilde{a}_2>0$). It is also important that at $\mu\neq 0$ the effective chiral couplings up to the second [see Eq. (7)] and the third nearest layers are present. This couplings have a significant effect on the magnitude of the phase angle α. It is shown below that when the effective chiral couplings between the nearest and the next nearest layers are opposing each other the region of stability of the Sm-C^*_α phase is significantly reduced compared to the case where $\tilde{f}_1$ and $\tilde{f}_2$ have the same sign. At fixed flexo (μ), piezo (c_{p0}) and electrostatic (b_0, b_1) interactions the sign of the effective parameter $\tilde{f}_1$ depends on the magnitude of the chiral model parameter f_{10} [see Eq. (6)]. Only minor changes in the magnitude of this parameter (i.e., minor changes in the molecular structure) can cause a change in the sign of $\tilde{f}_1$ which then essentially leads to a significant reduction or enlargement of the stability region of the Sm-$C^\star_\alpha$ phase as shown in Fig. 4.

In Figs. 4(a) and 4(b) phase diagrams are shown for materials which differ in the magnitude of the chiral model parameter f_{10}. In the phase diagram shown in Fig. 4(a) the effective chiral couplings between the nearest and the next nearest layers prefer the opposite helicoidal modulation and are thus opposing each other. In this case the stability of the Sm-C^*_α phase is limited to the region of optical purity where the general condition for the stability of the Sm-$C^\star_\alpha$ phase ($4|\tilde{a}_1|<\tilde{a}_2$) is satisfied. If the parameter f_{10} is slightly increased [Fig. 4(b)] the effective chiral couplings favor the same sense of the helicoidal modulation. So even in the region where the general condition for the stability of the Sm-$C^\star_\alpha$ phase is not satisfied, the helicoidal modulation is so large that the structure might be recognized as the Sm-$C^\star_\alpha$ phase.

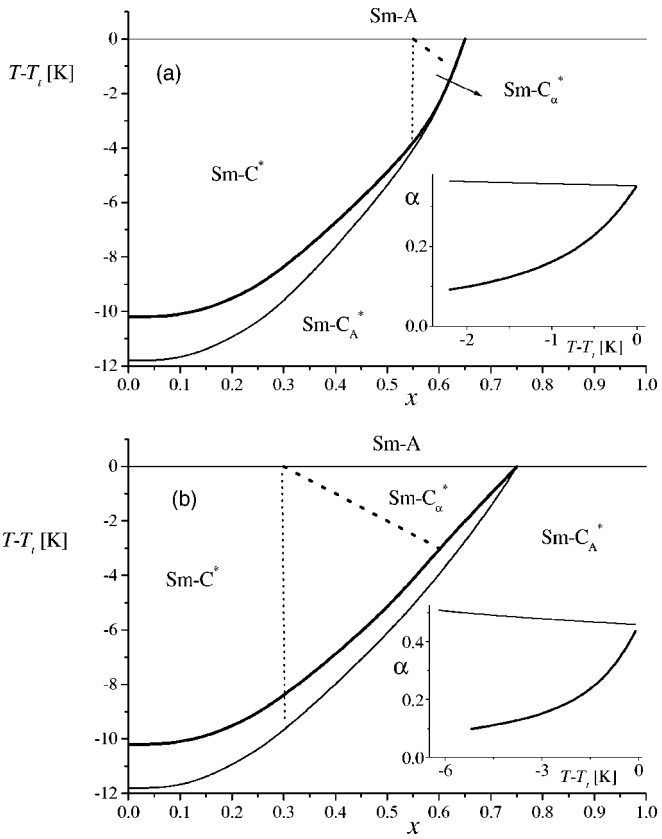

FIG. 4. Phase diagrams at finite flexoelectric coupling: the effect of the sign of the effective chiral coupling and the magnitude of the quadratic coupling. (a) $\tilde{f}_1=-\tilde{f}_2=0.06x$; the inset: $\alpha(T)$ at $x=0.6$. (b) $\tilde{f}_1=\tilde{f}_2=-0.06x$; the inset: $\alpha(T)$ at $x=0.5$. Both graphs: thin solid and dotted line: $b_Q=-2$; thick solid and dotted line: $b_Q=-10$. Solid and dotted lines on the phase diagrams denote the discontinuous and the continuous transitions, respectively. The common set of parameters: $\mu=0.3$, $c_p=4x$, $b=120$, $a_{10}=-0.4$, $a_{11}=4$, $b_0=2$, and $b_1=b_0/10$.

In Figs. 4(a) and 4(b) we also show the effect that the increased quadratic coupling has on the phase diagram. Since quadratic coupling enforces synclinic or anticlinic phases the region of stability of the Sm-$C^\star_\alpha$ phase is reduced. The Sm-$C^\star$ phase is pushed towards higher optical purity and in a certain region of optical purity one obtains the following phase sequence: Sm-$A\rightarrow$Sm-$C^\star_\alpha\rightarrow$Sm-$C^\star\rightarrow$Sm-$C^\star_A$ upon lowering the temperature. In the phase diagrams shown in Fig. 4 the phase transitions Sm-$C^\star\rightarrow$Sm-$C^\star_A$ and Sm-$C^\star_\alpha\rightarrow$Sm-$C^\star_A$ are discontinuous and the phase transition Sm-$C^\star_\alpha\rightarrow$Sm-$C^\star$ is continuous. However, the type of transition depends strongly on the strength of the piezo and flexoelectric coupling and on the effective chiral coupling between the nearest layers. In Fig. 5 we show the phase diagrams which are obtained if the flexoelectric and the effective chiral coupling are increased and the piezoelectric coupling is reduced. At low quadratic coupling one can expect the phase diagram shown in Fig. 5(a). The phase transition Sm-$C^\star_\alpha\rightarrow$Sm-$C^\star_A$ has become continuous and the phase transition Sm-$C^\star\rightarrow$Sm-$C^\star_A$ remains discontinuous. Additionally we have a discontinuous transition Sm-$C^\star\rightarrow$Sm-$C^\star_\alpha$ at

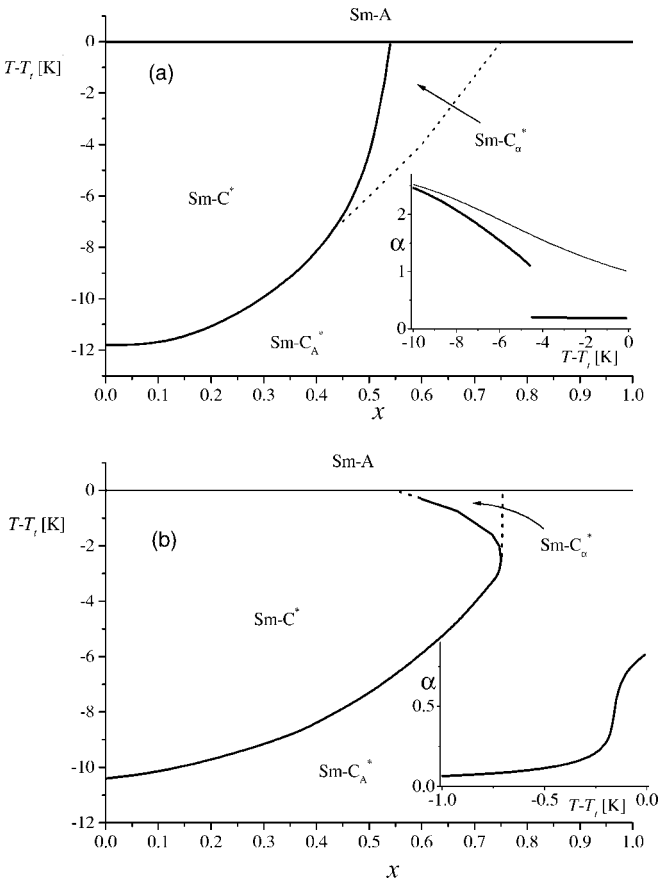

FIG. 5. Phase diagrams at $\mu=0.5$, $c_p=-3x$, $\tilde{f}_1=-0.17x$, and $\tilde{f}_2=0.075x$. The rest of the parameters are the same as in Fig. 4. (a) $b_Q=-2$; the inset: $\alpha(T)$ at $x=0.5$ (thick line) and at $x=0.6$ (thin line). (b) $b_Q=-10$; the inset: $\alpha(T)$ at $x=0.57$: the transition from the Sm-$C^\star_\alpha$ phase to the Sm-$C^\star$ is continuous. Both phase diagrams: solid and dotted lines denote the discontinuous and the continuous phase transitions, respectively. The Sm-$C^\star_\alpha$ phase is designated to the region in which $\alpha<1.5$.

$0.45<x<0.55$. If the quadratic coupling is increased the stability region of the Sm-$C^\star$ phase increases at the expense of the Sm-$C^\star_\alpha$ phase [see Fig. 5(b)]. The diagram is similar to the one shown in Fig. 4(b), but the phase transition from the Sm-$C^\star_\alpha$ to the Sm-$C^\star$ has become discontinuous. Only in a small range of optical purity the transition is still continuous. The variation of the phase angle with temperature is shown in Fig. 6. At low temperatures tilts in the neighboring layers are anticlinic and slightly distorted from the antiparallel orientation, which is typical for the Sm-$C^\star_A$ phase. Upon heating the structure discontinuously transforms into the synclinic helicoidally modulated structure of the Sm-$C^\star$ phase. Close to the transition temperature to the nontilted phase the phase difference again changes discontinuously and the helicoidally modulated structure with a short pitch, i.e., the Sm -$C^\star_\alpha$ phase, becomes stable.

The phase diagrams shown in Figs. 4 and 5 are again generic. They can be stretched or compressed in the horizontal direction by a simple rescaling of the piezoelectric parameter c_{p0} and the chiral model parameter f_{10}. For example, if both parameters are increased by a factor of 1.5, the "elbow"

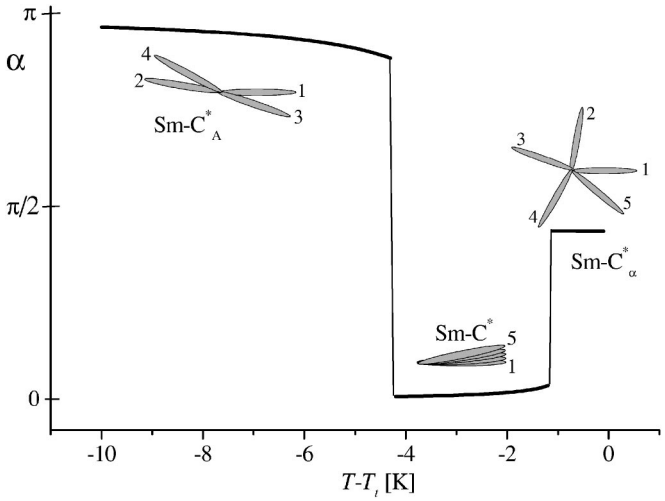

FIG. 6. Temperature dependence of the phase angle α at $x=0.7$ for the phase diagram shown in Fig. 5(b). At this optical purity all three clock phases are observed when temperature is reduced below the transition temperature T_t to the tilted phase. All the transitions are discontinuous. A schematic diagram (top view on the layers) is shown for each phase. The numbers count the successive layers.

of the Sm-$C^\star$ phase in Fig. 5(b) would extend to $x>1$, which means, that in the optically pure sample ($x=1$) one would observe the following phase sequence upon lowering the temperature: Sm-$A\rightarrow$Sm-$C^\star_\alpha\rightarrow$Sm-$C^\star\rightarrow$Sm-$C^\star_A$ and this would agree with the schematic diagram shown in Fig. 1(c). As already mentioned the rescaling of the diagram shown in Fig. 3(b) also gives a phase diagram which qualitatively agrees with the one on Fig. 1(c), however the origin of the Sm-$C^\star_\alpha$ phase in Figs. 3 and 5 is different.

IV. CONCLUSIONS

The discrete phenomenological model [17] reproduces the general phase diagrams that are consistent with the experimental results [15]. We have shown that the reduction of optical purity can change the effective coupling between the neighboring layers thus forcing the system from the antiferroelectric to the ferroelectric phase with a possible Sm-$C^\star_\alpha$ phase between them.

From the experimental phase diagrams one can predict which phenomenological parameters are the most important for the studied material and also conclude about their sign. If the phase diagram includes only two phases, Sm-$C^\star$ and Sm-$C^\star_A$, the flexoelectric coupling is very small. The materials which exhibit the Sm-$C^\star_\alpha$ phase in a certain range of optical purity and temperature, can be expected to have a large chiral model parameter f_{10} or/and the flexoelectric coupling that is comparable with the piezoelectric coupling. When temperature is lowered, the phase sequence Sm-$A\rightarrow$Sm-$C^\star_\alpha\rightarrow$Sm-$C^\star\rightarrow$Sm-$C^\star_A$ is possible in materials in which quadratic coupling is very strong. The transitions can be discontinuous only if flexoelectric coupling is significant as well. However, one should keep in mind that in such materials the intermediate phases Sm-$C^*_{FI,I}$ and Sm-$C^*_{FI,II}$

with a short modulation over three and four layers are usually present as well [7,15]. We have also shown that the phase transition from the Sm-$C^{\star}_{\alpha}$ phase to the Sm-$C^{\star}$ can be either continuous or discontinuous, depending on the optical purity [see Fig. 5(b)] as already experimentally observed [11].

We conclude by pointing out that the proposed model gives a possible explanation for the perplexing experimental evidence that the Sm-$C^{\star}_{\alpha}$ phase in some materials does not exist in optically pure samples, however if optical purity is reduced, this phase can be observed. According to the presented model the reduction of optical purity affects the magnitude of the inlayer polarization, as a result the interlayer electrostatic interactions change and this affects the effective interlayer interactions which depend on the electrostatic and the steric effects.

[1] A. D. L. Chandani, E. Gorecka, Y. Ouchi, H. Takezoe, and A. Fukuda, Jpn. J. Appl. Phys., Part 2 **28**, L1265 (1989); E. Gorecka, A. D. L. Chandani, Y. Ouchi, H. Takezoe, and A. Fukuda, Jpn. J. Appl. Phys., Part 1 **29**, 131 (1990).

[2] Y. Galerne and L. Liebert, Phys. Rev. Lett. **64**, 906 (1990).

[3] K. Hiraoka, Y. Takanishi, K. Skarp, H. Takezoe, and A. Fukuda, Jpn. J. Appl. Phys., Part 2 **30**, L1819 (1991).

[4] Ch. Bahr and D. Fliegner, Phys. Rev. Lett. **70**, 1842 (1993).

[5] A. Fokuda, Y. Takanishi, T. Isozaki, K. Ishikawa, and H. Takezoe, J. Mater. Chem. **4**, 997 (1994).

[6] P. Mach, R. Pindak, A.-M. Levelut, P. Barois, H. Nguyen, C. Huang, and L. Furenlid, Phys. Rev. Lett. **81**, 1015 (1998).

[7] M. Čepič, E. Gorecka, D. Pociecha, B. Žekš, and H. T. Nguyen, J. Chem. Phys. **117**, 1817 (2002).

[8] E. Gorecka, D. Pociecha, M. Čepič, B. Žekš, and R. Dabrowski, Phys. Rev. E **65**, 061703 (2002).

[9] C. W. Garland, Thermochim. Acta **88**, 127 (1985).

[10] M. Škarabot, M. Čepič, B. Žekš, R. Blinc, G. Heppke, A. V. Kityk, and I. Muševič, Phys. Rev. E **58**, 575 (1998).

[11] M. Škarabot and I. Muševič (unpublished).

[12] T. Isozaki, H. Takezoe, A. Fukuda, Y. Suzuki, and I. Kawamura, J. Mater. Chem. **4**, 237 (1994).

[13] H. Takezoe (private communication).

[14] J. P. F. Lagerwall, P. Rudquist, S. T. Lagerwall, and F. Giesselmann, Liq. Cryst. **30**, 399 (2003).

[15] H. Takezoe, in *Chirality in Liquid Crystals*, edited by J. Kitzerov and Ch. Bahr (Springer, New York, 2001), p. 271.

[16] H. Takezoe, J. Lee, A. D. L. Chandani, E. Gorecka, Y. Ouchi, A. Fukuda, K. Terashima, and K. Furukawa, Ferroelectrics **114**, 187 (1991); A. D. L. Chandani, Y. Ouchi, H. Takezoe, A. Fukuda, K. Terashima, K. Furukawa, and A. Kishi, Jpn. J. Appl. Phys., Part 2 **28**, L1261 (1989).

[17] M. Čepič and B. Žekš, Phys. Rev. Lett. **87**, 085501 (2001).

[18] D. J. Photinos and E. T. Samulski, Science **270**, 783 (1995).

[19] M. P. Neal, A. J. Parker, and C. M. Care, Mol. Phys. **91**, 603 (1997).

[20] D. Pociecha, E. Gorecka, M. Čepič, N. Vaupotič, B. Žekš, D. Kardas, and J. Mieczkowski, Phys. Rev. Lett. **86**, 3048 (2001).

[21] A. V. Emelyanenko and M. A. Osipov, Phys. Rev. E **68**, 051703 (2003).

[22] M. Čepič and B. Žekš, Mol. Cryst. Liq. Cryst. Sci. Technol., Sect. A **301**, 221 (1997).

[23] A. G. Petrov and A. Derzhanski, Mol. Cryst. Liq. Cryst. **151**, 303 (1987).

[24] J. Gruler, J. Chem. Phys. **61**, 5408 (1974).